Optimization of Seating Position and Stimulation Pattern in Functional Electrical Stimulation Cycling: Simulation Study

Ehsan Jafari†, Efe A.Aksoez, Petar Kajganic, Amine Metani, Lana Popovic-Maneski, and Vance Bergeron

***Abstract*— Two significant challenges facing functional electrical stimulation (FES) cycling are the low power output and early onset of muscle fatigue, mainly due to the non-physiological and superficial recruitment of motor units and weakness of the antagonistic muscles. Thus optimization of the cycling biomechanical properties and stimulation pattern to achieve maximum output power with minimum applied electrical stimulus is of great importance. To find the optimal seating position and stimulation pattern, the previous works either ignored the muscle's force-velocity and force-length properties or employed complicated muscle models which was a massive barrier to clinical experiments. In this work, an easy-to-use and precise muscle model in conjunction with Jacobian-based torque transfer functions were adopted to determine the optimal seating position, trunk angle, crank arm length, and stimulation intervals. Furthermore, the impact of muscle force-velocity factor in finding the optimal seating position and stimulation intervals was investigated. The simulation models showed the trivial effect of the force-velocity factor on the resulting optimal seating position of six healthy simulated subjects. This method can enhance the FES-cycling performance and shorten the time-consuming process of muscle model identification for optimization purposes.**

***Index Terms*—optimization, FES-cycling, stimulation pattern, seating position**

I. Introduction

Spinal cord injury (SCI) stems from traumatic damages (e.g., fall, vehicle accident) or non-traumatic damages (e.g., infections) to the spinal cord, which will result in a change, either temporary or permanent, in its normal function [1]. Lower limb paralysis (complete or incomplete) or paraplegia is one of the expected devastating consequences of spinal cord injury, forcing the affected person to depend on other people such as family members or caregivers to accomplish the activities of daily living. Due to the sedentary lifestyle, people with paraplegia are susceptible to cardiovascular disease, bedsores, urinary tract infections, bone demineralization, and muscle atrophy [2].

Applying low-level electrical stimulation by surface or implanted electrodes can elicit contractions in the skeletal muscles of patients with intact lower motor neurons. The electrical impulses can functionally trigger the muscle groups to induce a certain kind of movement, such as cycling, rowing, standing, or even walking. In contrast to walking, cycling is performed in a seated position which means that the patient is not in danger of sudden fall and bone fracture. Moreover, paralyzed muscles might not be so strong at the beginning of rehabilitation to be involved in walking training. For cycling, the patient is less dependent on family or clinic staff, and it can be even more enjoyable in the case of non-stationary outdoor cycling. FES-cycling has various health benefits such as improving cardiovascular and pulmonary functions, peripheral circulation, muscle bulk and strength, gas exchange kinetics, and aerobic metabolism [3], [4].

Even though the beneficial health outcomes of FES for motor-impaired individuals are extensively documented, two significant unresolved limitations confine the development of this method as global rehabilitation therapy. The significantly lower power generated by FES cycling than volitional cycling and the early onset of muscular fatigue limit the exercise duration [5]. The main reason behind these shortcomings is the non-physiological and superficial recruitment of motor units and the weakness of the antagonistic muscles [6]. To be more detailed, the motor unit recruitment pattern in natural contractions follows the Henneman's size principle [26], which means that motor units are recruited in size from small and slow to large and fast. In contrast, this order is not followed by surface electrical stimulation [7], [8]. These points enlighten the significance of optimizing the cycling biomechanical properties to achieve maximum output power with minimum applied electrical stimulus. Previous works focused on different aspects such as enhancing the mechanical structure of the ergometer [9]-[12], investigating the effects of changing the geometrical distances (e.g., seating position), and pedaling rate [12], [15], and finding optimum stimulation pattern of muscle groups [13], [16],

In [13], the muscle group torque transfer ratio was used to determine the ON and OFF times for stimulation of the gluteal, quadriceps, and hamstrings muscles. In this method, the length of leg segments of each patient and geometric properties of the stationary recumbent cycle were measured to determine each muscle group transfer ratio. The stimulation for each muscle group was ON only when the corresponding Jacobian element was greater than a threshold value determined by the trial-and-error method.

*Research supported by Kurage.

†Corresponding author.

E. Jafari, P. Kajganic, A. Metani and V. Bergeron are with CNRS UMR 5672, Ecole Normale Supérieure de Lyon, 46 allée d'Italie, 69007, Lyon, France (email: ehsan.jafari@ens-lyon.fr; petar.kajganic@ens-lyon.fr; amine.metahni@ens-lyon.fr; vance.bergeron@ens-lyon.fr).

E. A. Aksoez is with Motor Learning and Neurorehabilitation Laboratory, ARTORG Center for Biomedical Engineering Research, University of Bern, Switzerland (email: efe.aksoez@unibe.ch)

L. P. Maneski is with Institute of Technical Sciences of SASA, Knez Mihailova 35/IV 11000 Belgrade, Serbia (email: lana.popovic.maneski@itn.sanu.ac.rs).

In [9], a complicated dynamic model of the musculoskeletal structure of lower limbs of a paraplegic patient and a simulated leg cycling system was developed. The proposed model evaluated the effects of seating position, stimulation pattern, and cycling loads on improving cycling efficiency. This study showed that adjusting the geometrical properties has a significant impact on the performance of the virtual patient. Nevertheless, their proposed results have not yet been verified on real subjects.

In [16], a model of electrically stimulated muscle was combined with equations of motion of lower limbs on an ergometer to obtain a theoretical framework for investigating the contribution of each stimulated muscle group in the crank torque and finding the optimal stimulation pattern. Their cost function considered the maximum power output generated by the lowest muscle force. Later in [14], they have investigated the influence of seating position and pedaling rate on the optimal stimulation pattern while pedaling on a non-circular path. Rasmussen et al., to eliminate the dead points of cycling, developed a four-bar linkage cycling mechanism by adding a lever arm and coupler [12]. They determined the optimal stimulation pattern that could propel the muscles to produce constant torque around the crank cycle with minimum possible muscle force.

To find the optimal seating position and stimulation pattern, the above-mentioned works either ignored the muscle's force-velocity and force-length properties or employed muscle models which are complex and time-consuming to be identified in clinics for actual SCI patients. Moreover, most rehabilitation centers use commercial ergometers, e.g., Ergys, MOTOmed, RT, which cannot provide a non-circular pedaling system or dead points-free cycling.

This study aims to propose a novel method to find the optimal position of the seat concerning the crank center, trunk angle of the user, and crank arm length while pedaling at the proper cadence for SCI patients. To meet this aim, an easy-to-use and precise model of the skeletal muscle was combined with the torque transfer functions of the lower body joints. Furthermore, the impact of muscle force (joint torque)-velocity (joint angular velocity) factor in finding the optimal point was investigated. As a beneficial corollary, an optimal stimulation interval for each active muscle group was determined based on the optimization functions. This method can be employed in most clinics with different ergometer types to help the patients to keep their exercise for a longer duration.

II. METHODS

A. Model of Skeletal Muscle

The force produced by skeletal muscle in response to natural or artificial electrical stimulation has three major components: the activation dynamics factor (recruitment curve, contraction dynamics), force (joint torque)-length (joint angle) factor, and force (joint torque)-velocity (joint angular velocity) factor [17]-[19]. The first component imitates the relationship between stimulation strength, recruited fibers, and output force. According to the sliding filament theory, there is an optimal sarcomere length at which muscle force reaches its maximum capacity, while at shorter and longer lengths, the force decays to zero with nonlinear behavior [20], [21]. In this work, the following model was selected for isometric joint torque-angle factor from [22]

$$A_{TA}\left(\theta\right)=\cos\left(\pi\frac{\theta-\theta_0}{\Delta\theta}\right) \tag{1}$$

where θ is the joint angle, θ_0 is the joint angle where maximum force is generated, and $\Delta\theta$ is the range of joint angle in which active muscle force occurs.

To model the joint torque-angular velocity factor, the modified Hill equation [23] was recruited from [22]

$$A_{TV}\left(\dot{\theta}\right)=\frac{2\omega_1\omega_2+\dot{\theta}\left(\omega_1-3\omega_2\right)}{2\omega_1\omega_2+\dot{\theta}\left(2\omega_1-4\omega_2\right)} \tag{2}$$

where ω_1 and ω_2 are the joint angular velocities at which muscle force reaches 50% and 75% of the isometric force. According to this equation, the force (torque) exerted by muscle decreases as the muscle shortening velocity increases.

This work assumes that stimulation intensity has its maximum possible value at each moment, so the activation dynamics factor is constant but still muscle-specific. Hence, combining (1) and (2) yields the final model for active muscle torque

$$T_{ACTIVE}\left(\theta,\dot{\theta}\right)=T_{MAX}A_{TA}\left(\theta\right)A_{TV}\left(\dot{\theta}\right) \tag{3}$$

where T_{MAX} is the maximum isometric joint torque. It should be mentioned that the moment arm which relates the muscle force to the corresponding joint torque is considered to be angle-independent for the sake of simplicity.

B. Model of stationary cycle

A planar model of a two-legged recumbent bike with lower limbs and trunk of a rider is presented in Fig. 1(a). This model consists of two closed kinematic chains for each leg connected at the hip joint and crank center. Each kinematic chain has four links (thigh, lower leg, crank arm, and frame of stationary cycle) and four revolute joints (hip, knee, pedal, and crank center). The cycle frame consists of a vertical segment and a horizontal segment that is fixed to the ground. The ankle joint is assumed to be fixed at 90° and rigidly connected to the pedal for lateral stability and safety of the rider. The proposed closed kinematic chains can be described entirely by the length of the links (l_{th} , l_l , l_{cr} , l_x , l_y) and crank angle of one side (q_r) due to the following constraints: i) hip and crank center are fixed, ii) pedals have a constant 180° of phase difference. To find q_h and q_k concerning the crank angle, each link of the closed kinematic chain (e.g., right side) can be considered a vector in the x-y plane as depicted in Fig. 1(b). Projecting each vector on the x- and y-axis yields

$$l_{cr}\cos\left(q_r\right)+l_l\cos(q_k)+l_{th}\cos(q_h)-l_x=0 \tag{4}$$

$$-l_{cr}\sin\left(q_r\right)-l_l\sin(q_k)+l_{th}\sin(q_h)+l_y=0 \tag{5}$$

solving these two independent equations for q_h and q_k in terms of q_r yields the following parametric solutions

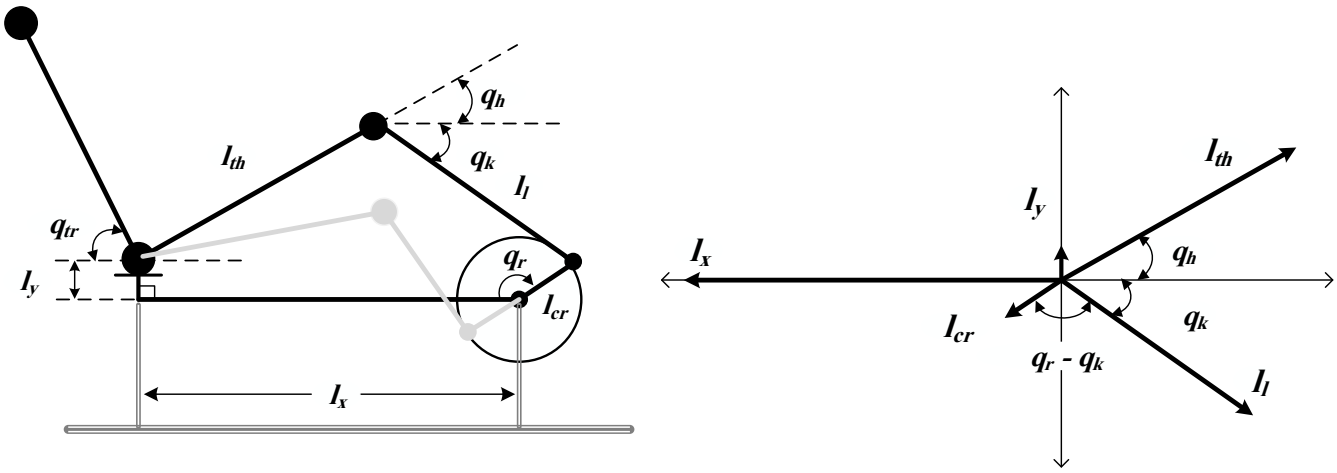

(a) (b)

Fig. 1. (a) Skeletal model of stationary cycling. q_r , q_{tr} , q_h , and q_k are the crank angle, the trunk angle, the angle between thigh and ground, and the angle between shank and ground, respectively. l_{cr} , l_{th} , l_l , l_x , and l_y are the crank arm length, the thigh length, the lower leg length, the horizontal distance between the hip joint and the crank center, and the vertical distance between the hip joint and crank center, respectively. (b) Projected view of skeletal model segments on x-axis and y-axis

$$q_h = \beta - \arccos\left(\frac{-\alpha_3}{\sqrt{\alpha_1^2 + \alpha_2^2}}\right) \tag{6}$$

$$q_k = -\arctan\left(\frac{-l_{cr}\sin(q_r) + l_{th}\sin(q_h) + l_y}{l_{cr}\cos(q_r) + l_{th}\cos(q_h) - l_x}\right) \tag{7}$$

where

$$\alpha_1 = -2l_{th}(l_{cr}\sin(q_r) - l_y)$$
$$\alpha_2 = 2l_{th}(l_{cr}\cos(q_r) - l_x)$$
$$\alpha_3 = l_x^2 + l_y^2 + l_{th}^2 - l_l^2 + l_{cr}^2 - 2l_{cr}(l_x\cos(q_r) + l_y\sin(q_r))$$
$$\beta = \pi + \arctan\left(\frac{\alpha_1}{\alpha_2}\right)$$

The left side has similar solutions with respect to $q_l = \pi + q_r$ [24].

As mentioned in the previous section, the force exerted by muscle contraction in response to the stimulation produces torque around the corresponding joint. This torque is transferred from the leg joints to the crank axis via the torque transfer functions to rotate the pedals and legs. Quadriceps femoris (knee extensor), hamstrings (knee flexor), and gluteal (hip extensor) muscle groups are the main force actuators in cycling exercise which can be easily stimulated by surface electrodes. Torque transfer functions from hip and knee joints to the crank center are defined as [24], [25]

$$J_h(q_r) = \frac{\partial\theta_h}{\partial q_r}, \quad J_k(q_r) = \frac{\partial\theta_k}{\partial q_r} \tag{8}$$

where $\theta_h = q_h + q_{tr}$, and $\theta_k = q_h + q_k$ are hip joint and knee joint angle, respectively. q_{tr} is the angle between the trunk of the subject and the ground, as depicted in Fig. 1(a). Since q_{tr} is constant during cycling motion, (8) can be rewritten as

$$J_h(q_r) = \frac{\partial q_h}{\partial q_r}, \quad J_k(q_r) = \frac{\partial(q_h + q_k)}{\partial q_r} \tag{9}$$

by taking the time derivative from (4) and (5) and considering

$$\dot{q}_h = \frac{\partial q_h}{\partial q}\dot{q}, \quad \dot{q}_k = \frac{\partial q_k}{\partial q}\dot{q} \tag{10}$$

(8) can be expressed in terms of q_r [24]

$$J_h(q_r) = \frac{l_{cr}}{l_{th}}\left(\frac{\sin(q_k - q_r)}{\sin(q_k + q_r)}\right) \tag{11}$$

$$J_k(q_r) = \frac{l_{cr}}{l_{th}}\left(\frac{\sin(q_k - q_r)}{\sin(q_k + q_r)}\right) - \frac{l_{cr}}{l_l}\left(\frac{\sin(q_h + q_r)}{\sin(q_k + q_r)}\right) \tag{12}$$

To elicit the torque transfer functions for the involved muscle groups, it should be noticed that clockwise torque about the crank axis is considered as positive torque. Hence (with respect to Fig. 1(a)), the muscle torque transfer function for each muscle group is determined as

$$J_{hams}(q_r) = \begin{cases} J_k(q_r) & \text{if } J_k(q_r) > 0 \\ 0 & \text{if } J_k(q_r) \le 0 \end{cases} \tag{13}$$

$$J_{quad}(q_r) = \begin{cases} 0 & \text{if } J_k(q_r) \ge 0 \\ -J_k(q_r) & \text{if } J_k(q_r) < 0 \end{cases} \tag{14}$$

$$J_{glut}(q_r) = \begin{cases} 0 & \text{if } J_h(q_r) \ge 0 \\ -J_h(q_r) & \text{if } J_h(q_r) < 0 \end{cases} \tag{15}$$

C. Optimization

Method 1: According to the previous sections, the force (joint torque)-length (joint angle) factor, the force (joint torque)-

TABLE I. SUMMARY OF SUBJECTS SPECIFICATIONS [22]

Subject	S1	S2	S3	S4	S5	S6
Gender	M	F	M	F	M	F
Age (years)	19.6	19.6	61.3	58.1	71.7	68.3
Height (cm)	174.8	160.6	174.7	162.6	174.3	161.7
Mass (kg)	72.8	62.1	87.7	66.0	86.2	64.5
l_{th} (cm)	42.82	39.34	42.80	39.83	42.70	39.61
l_l (cm)	49.81	45.77	49.78	46.34	49.67	46.08

velocity (joint angular velocity) factor, and the torque transfer functions of the stimulated muscle groups have a pivotal role in obtaining the maximum forward torque about the crank from the provided electrical stimulation. Multiplication of these factors for each muscle group is defined as the muscle optimization function

$$\delta_m^1(q_r) = T_{MAX}^m \cdot A_{TA}^m(\theta_j(q_r)) \cdot A_{TV}^m(\dot{\theta}_j(q_r)) \cdot J_m(q_r) \tag{16}$$

where $m \in M \equiv \{hams, quad, glut\}$ indicates muscle group. The final optimization function which should be maximized is constructed by taking integral of the muscle optimization functions (16) over a whole crank cycle for each muscle group and adding them together

$$\psi_1 = \sum_{m \in M} \int_0^{2\pi} \delta_m^1(q_r) dq_r \tag{17}$$

Method 2: Finding the parameters of (2) for three muscle groups of each subject is time-consuming and tedious. Moreover, the required tests to determine muscle shortening velocities at which muscle force reaches 50% and 75% of the isometric force may lead to early onset of muscle fatigue in paralyzed muscles. In this mode, we omitted the torque-angular velocity factor from (16) and defined the muscle optimization function as

$$\delta_m^2(q_r) = T_{MAX}^m \cdot A_{TA}^m(\theta_j(q_r)) \cdot J_m(q_r) \tag{18}$$

Thus the final optimization function is

$$\psi_2 = \sum_{m \in M} \int_0^{2\pi} \delta_m^2(q_r) dq_r \tag{19}$$

D. Constraints

As depicted in Fig. 1(a), the thigh segment, the lower leg segment, and the imaginary line which connects the hip joint to the pedal (l_b) are sides of an imaginary triangle. According to the triangle inequality, the following conditions must be satisfied over a crank cycle

$$\begin{aligned} l_l + l_{th} &> \max(l_b) \\ l_l - l_{th} &< \min(l_b) \end{aligned} \tag{20}$$

TABLE II. THE MUSCLE MODEL PARAMETERS OF AVERAGED SUBJECTS [22]

Muscle Groups	Muscle Parameters	S1	S2	S3	S4	S5	S6
Hip Extensor	T_{MAX} [a]	0.161	0.181	0.171	0.140	0.144	0.138
	θ_0 (rad)	0.932	1.242	1.176	1.241	1.125	1.542
	$\pi/\Delta\theta$	0.958	0.697	0.922	0.830	0.896	0.707
	ω_1 (rad/s)	1.578	1.567	1.601	1.444	1.561	1.613
	ω_2 (rad/s)	3.190	3.164	3.236	2.919	3.152	3.256
Knee Extensor	T_{MAX} [a]	0.163	0.159	0.156	0.128	0.137	0.124
	θ_0 (rad)	1.133	1.274	1.173	1.141	1.067	1.140
	$\pi/\Delta\theta$	1.258	1.187	1.225	1.286	1.310	1.347
	ω_1 (rad/s)	1.517	1.393	1.518	1.332	1.141	1.066
	ω_2 (rad/s)	3.952	3.623	3.954	3.469	3.152	2.855
Knee Flexor	T_{MAX} [a]	0.087	0.080	0.081	0.060	0.069	0.060
	θ_0 (rad)	0.522	0.635	0.523	0.402	0.437	0.445
	$\pi/\Delta\theta$	0.869	0.873	0.986	0.967	0.838	0.897
	ω_1 (rad/s)	2.008	1.698	1.830	1.693	1.718	1.121
	ω_2 (rad/s)	5.233	4.412	4.777	4.410	4.476	2.922

a. Values are normalized by body weight × height

The extremum values of l_b calculated with respect to l_x, l_y, and l_{cr} as

$$\begin{aligned} \max(l_b) &= \sqrt{{l_{cr}}^2 + {l_x}^2 + {l_y}^2 + 2l_{cr}\sqrt{{l_x}^2 + {l_y}^2}} \\ \min(l_b) &= \sqrt{{l_{cr}}^2 + {l_x}^2 + {l_y}^2 - 2l_{cr}\sqrt{{l_x}^2 + {l_y}^2}} \end{aligned} \tag{21}$$

The optimization ranges for l_x and l_y were

$l_x \in [lb_x, ub_x]$, $l_y \in [lb_y, ub_y]$

where $lb_x = l_{cr}$, $ub_x = l_{th} + l_l - l_{cr}$, $lb_y = 0$, and $ub_y = l_{th} + l_l - l_{cr}$. The upper bounds correspond to full knee extension while $l_y = 0$ and $l_x = 0$, respectively.

The optimization ranges for l_{cr} and q_{tr} were $l_{cr} \in [10, 40]$, $q_{tr} \in [0, \pi/2]$ which were selected from the literature [9].

To prevent knee joint hyper-extension, the maximum knee joint extension angle was taken as 165° [12]. The cycling cadence was considered 35 RPM as cycling at higher rates makes the SCI subject feel uncomfortable and increases spasm activities [12], [14].

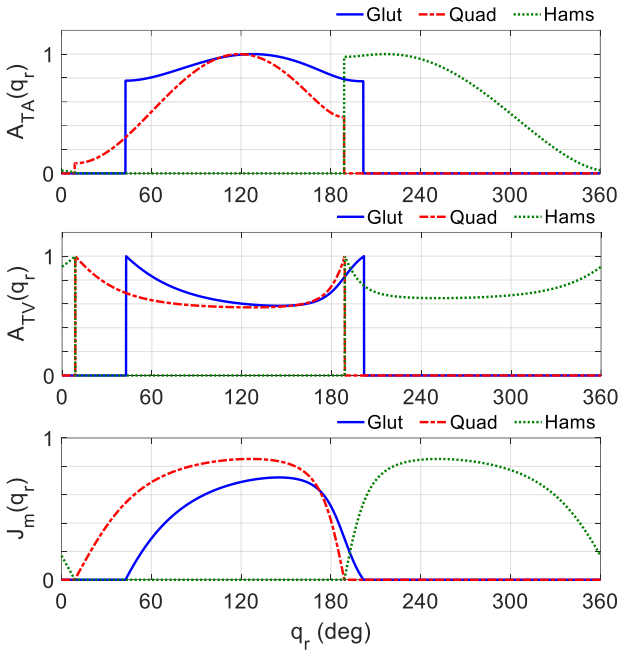

Fig. 2. Torque-angle factor, torque-angular velocity factor, and torque transfer functions of gluteal, quadriceps, and hamstrings muscle groups using optimized values of S1.

III. Results

In [22], 34 healthy subjects were classified by their gender (male (17 subjects), female (17 subjects)) and age range (18-25 (14 subjects), 55-65 (14 subjects), and over 65 (6 subjects)) in six groups. The subject's specifications including age, gender, height, and mass, were averaged over each group and considered as specifications of an averaged subject. The humanoid dimensions (length of thigh and lower leg with respect to height) utilized here are extracted from the standard anthropometric human measurements introduced in [21]. A summary of the specifications of six averaged subjects is presented in Table I.

The muscle model parameters corresponding to three muscle groups (gluteal as hip extensor, quadriceps as knee extensor, and hamstrings as knee flexor) of six averaged subjects were extracted from [22] and summarized in Table II.

TABLE III. Optimization variables, range, step size, and optimized seating variables measured by Method 1 and Method 2.

Var.	Range (Step Size)	Method	S1	S2	S3	S4	S5	S6
l_x (cm)	$lb_x - ub_x$ (1)	1	64	57	63	63	66	62
		2	64	57	63	63	65	62
l_y (cm)	$lb_y - ub_y$ (1)	1	10	6	30	21	8	11
		2	10	6	30	21	14	11
l_{cr} (cm)	10-40 (1)	1	27	27	22	19	25	22
		2	27	27	22	19	25	22
q_{tr} (rad)	0-1.57 (0.05)	1	0.25	0.45	0.90	0.85	0.45	0.95
		2	0.25	0.45	0.90	0.90	0.55	0.95

The parameters for which the optimization was performed included the vertical distance between the hip joint and crank center (l_y), the horizontal distance between the hip joint and crank center (l_x), crank arm length (l_{cr}), and the angle between the trunk of the subject and the ground (q_{tr}). The optimization range and step size of parameters are presented in Table III. The muscle model and the optimization process were implemented in MATLAB (The MathWorks Inc., USA). The optimization process was performed for both proposed methods, and the optimal values are presented in Table III. It is observed that the resulting optimal values from the two methods are precisely similar for S1, S2, S3, and S6. The optimal values for S5 and S6 show a slight difference between the two methods.

Torque-angle factor, torque-angular velocity factor, and torque transfer functions of gluteal, quadriceps, and hamstrings muscle groups using optimized values of S1 are illustrated in Fig. 2.

Root Mean Square (RMS) error was utilized to evaluate the similarity between muscle optimization functions resulting from Method 1 and 2. The muscle optimization functions were normalized for ease of comparison. The results of both methods for S1 and S5 are illustrated in Fig. 3 and Fig. 4, respectively. Table IV summarizes the accuracy of both methods for three muscle groups. It is observed that the averaged errors of Method 2 in estimating the muscles optimization functions corresponding to Method 1 are 5.28±1.21%, 3.16±1.19%, and 3.29±2.15% for gluteal, quadriceps, and hamstrings, respectively.

The muscle optimization function can also provide efficient stimulation intervals for each muscle group. Indeed, each muscle group should be stimulated at the angles with large muscle optimization function values. This can be performed by considering a minimum threshold (e.g., 0.5) for

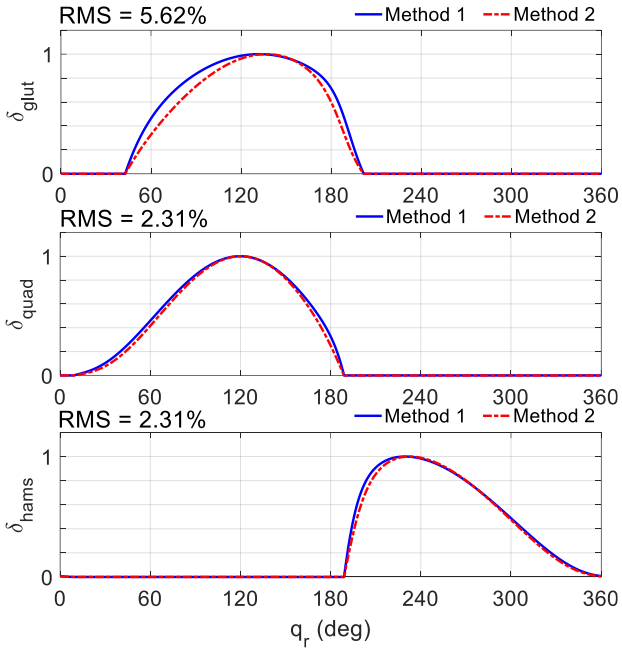

Fig. 3. Normalized muscle optimization function of gluteal, quadriceps, and hamstrings over a whole crank cycle for S1 using optimal seating position resulted from Method 1 and Method2.

TABLE IV. STIMULATION INTERVALS MEASURED FROM NORMALIZED MUSCLE OPTIMIZATION FUNCTIONS GREATER THAN THRESHOLD VALUE OF 0.5 USING METHOD 1 AND METHOD 2. NORMALIZED MUSCLE OPTIMIZATION FUNCTION ESTIMATION ERROR OF METHOD 2 FOR THREE MUSCLE GROUPS AND SIX AVERAGED SUBJECTS.

Subjects	Muscle Group	glut		quad		hams	
	Method	Stimulation Interval (rad)	Accuracy (RMS%)	Stimulation Interval (rad)	Accuracy (RMS%)	Stimulation Interval (rad)	Accuracy (RMS%)
S1	1	[1.08-3.27]	5.62%	[1.09-3.00]	2.31%	[3.41-5.21]	2.31%
	2	[1.24-3.20]		[1.14-2.95]		[3.45-5.19]	
S2	1	[1.18-3.27]	5.47%	[1.11-2.95]	2.06%	[3.36-5.11]	2.32%
	2	[1.34-3.19]		[1.14-2.90]		[3.39-5.11]	
S3	1	[1.55-3.58]	4.73%	[1.22-3.27]	3.09%	[3.70-5.62]	2.48%
	2	[1.71-3.52]		[1.32-3.23]		[3.74-5.57]	
S4	1	[1.47-3.45]	4.41%	[1.05 ,3.14]	3.31%	[3.59-5.54]	2.56%
	2	[1.61-3.40]		[1.16 ,3.10]		[3.62-5.48]	
S5	1	[1.16-3.26]	7.42%	[1.01-2.96]	5.39%	[3.38-5.22]	7.67%
	2	[1.42-3.28]		[1.16-3.01]		[3.51-5.28]	
S6	1	[1.56-3.33]	4.03%	[1.01-3.01]	2.79%	[3.43-5.31]	2.39%
	2	[1.67-3.28]		[1.09-2.96]		[3.47-5.27]	
Average ± SD (%)			5.28±1.21%		3.16±1.19%		3.29±2.15%

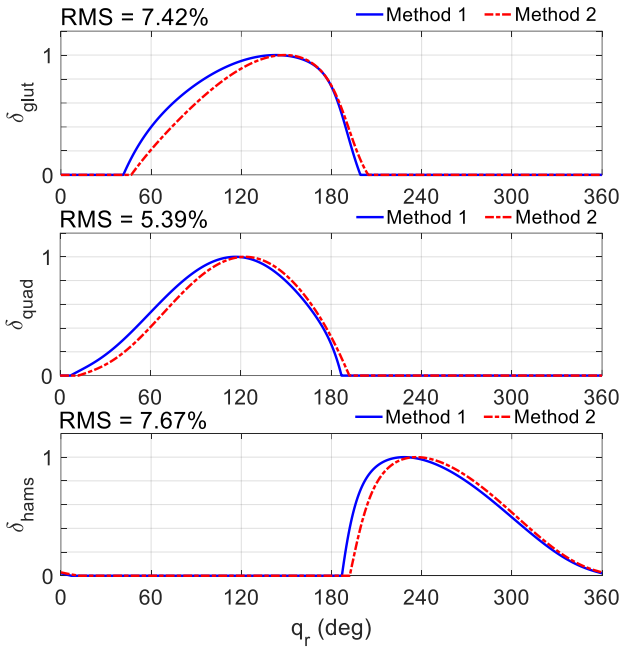

Fig. 4. Normalized muscle optimization function of gluteal, quadriceps, and hamstrings over a whole crank cycle for S5 using optimal seating position resulted from Method 1 and Method2.

each normalized muscle optimization function and turning the stimulation on for angles with greater than threshold values as presented in Table IV.

IV. DISCUSSION AND CONCLUSION

In this work, two optimization schemes were developed to determine the seating position for which the maximum crank torque is achieved from the provided stimulation during indoor recumbent FES-cycling. The proposed schemes relied on the muscle model and torque transfer ratio to find the optimal seating position from the muscle to the crank. Despite the first method, which required a complete identification of isometric and isokinetic terms of a muscle model, the second method only relied on the isometric part. According to the results, the second method can determine the optimal seating position and stimulation intervals with excellent accuracy, mainly attributed to the low pedaling rates in SCI patients. This work considered a cycling cadence of 35 RPM, which corresponds to a comfortable pedaling rate that SCI patients should be able to achieve without problems [12]. This relatively low cadence was selected because experiments have shown that patients start to feel uncomfortable, and spasm activity increases at above 35 rpm cadences [12]. Using the proposed method can shortcut the time-consuming process of muscle identification to find the proper seating position and help the patients to use the maximum strength of their muscles which leads to more exercise duration and efficiency.

Although the proposed method showed promising results, there are still some limitations that should be considered. First of all, the specifications of the simulated muscle model were extracted from healthy subjects during voluntary joint torque production, while the proposed optimizations were designed to determine the best seating position and stimulation interval for electrically induced cycling. It should also be noticed that the torque produced by SCI patients is only due to the electrical stimulation. Conversely, in healthy subjects, there are two components of activation (hybrid) during FES-cycling: one volitional and one induced and the analysis is quite distinct [27].

The finding that the force-velocity factor does not have a significant effect on the optimal position of the lower limb during cycling may be due to the fact that the cost function has not considered muscle energy consumption during cycling. Considering this factor in the cost function or another round of optimization after determining the optimal seating position should be employed to determine the optimal speed of cycling in which the factor of force-velocity may have a dominant role.

Artificial electrical stimulation can only stimulate large and superficial muscle groups, leading to low muscle force and early onset of fatigue. The proposed approach is able to

prescribe an optimal muscle activation pattern that can mitigate the problem of muscle fatigue during FES-cycling. But it does not prevent the issues pertaining to surface electrical stimulation, such as reversed recruitment order and poor spatial selectivity in activating the motor nerves. Moreover, the proposed optimization method is not capable of finding the optimal amount of electrical stimulation that should be provided to the muscle to reduce the fatigue effect.

The bi-articular behavior of muscles, such as the biceps femoris, means that torque around one joint depends on another joint's position. Bi-articular muscles were not considered in the current model due to complexity. We will investigate the effect of these limitations and the efficiency of the proposed optimization method with actual SCI patients in our future work.

REFERENCES

[1] C. S. Ahuja *et al.*, "Traumatic spinal cord injury," *Nat. Rev. Dis. Primers*, vol. 3, no. 1, p. 17018, 2017.

[2] R. Sweis and J. Biller, "Systemic complications of spinal cord injury," *Curr. Neurol. Neurosci. Rep.*, vol. 17, no. 1, 2017.

[3] C.-W. Peng, S.-C. Chen, C.-H. Lai, C.-J. Chen, C.-C. Chen, J. Mizrahi, and Y. Handa, "Review: Clinical benefits of functional electrical stimulation cycling exercise for subjects with central neurological impairments," *J. Med. Biol. Eng.*, vol. 31, pp. 1–11, Jan. 2011.

[4] C. Fattal, B. Sijobert, A. Daubigney, E. Fachin-Martins, B. Lucas, J.-M. Casillas, and C. Azevedo, "Training with FES-assisted cycling in a subject with spinal cord injury: Psychological, physical and physiological considerations," *J. Spinal Cord Med.*, vol. 43, no. 3, pp. 402–413, 2018.

[5] K. J. Hunt, J. Fang, J. Saengsuwan, M. Grob, and M. Laubacher, "On the efficiency of FES cycling: a framework and systematic review," *Technol. Health Care*, vol. 20, no. 5, pp. 395–422, 2012.

[6] J. Szecsi, A. Straube, and C. Fornusek, "A biomechanical cause of low power production during FES cycling of subjects with SCI," *J. Neuroeng. Rehabil.*, vol. 11, no. 1, p. 123, 2014.

[7] P. H. Gorman and J. T. Mortimer, "The effect of stimulus parameters on the recruitment characteristics of direct nerve stimulation," *IEEE Trans. Biomed. Eng.*, vol. 30, no. 7, pp. 407–414, 1983.

[8] F. Rattay, "Modeling the excitation of fibers under surface electrodes," *IEEE Trans. Biomed. Eng.*, vol. 35, no. 3, pp. 199–202, 1988.

[9] L. M. Schutte, M. M. Rodgers, F. E. Zajac, and R. M. Glaser, "Improving the efficacy of electrical stimulation-induced leg cycle ergometry: an analysis based on a dynamic musculoskeletal model," *IEEE Trans. Rehabil. Eng.*, vol. 1, no. 2, pp. 109–125, 1993.

[10] S. C. Abdulla, O. Sayidmarie, and M. O. Tokhi, "Functional electrical stimulation-based cycling assisted by flywheel and electrical clutch mechanism: A feasibility simulation study," *Rob. Auton. Syst.*, vol. 62, no. 2, pp. 188–199, 2014.

[11] T. Angeli, M. Gföhler, T. Eberharter, P. Lugner, and L. Rinder, "Optimiziation of the pedal path for cycling powered by lower extremity muscles activated by functional electrostimulation FES," *Comp. Meth. Biomech. Biomed. Eng.*, vol. 3, pp. 263–268, 2001.

[12] J. Rasmussen, S. T. Christensen, M. Gföhler, M. Damsgaard, and T. Angeli, "Design optimization of a pedaling mechanism for paraplegics," *Struct. Multidiscipl. Optim.*, vol. 26, no. 1–2, pp. 132–138, 2004.

[13] M. J. Bellman, T.-H. Cheng, R. J. Downey, C. J. Hass, and W. E. Dixon, "Switched control of Cadence during stationary cycling induced by functional electrical stimulation," *IEEE Trans. Neural Syst. Rehabil. Eng.*, vol. 24, no. 12, pp. 1373–1383, 2016.

[14] M. Gföhler and P. Lugner, "Dynamic simulation of FES-cycling: influence of individual parameters," *IEEE Trans. Neural Syst. Rehabil. Eng.*, vol. 12, no. 4, pp. 398–405, 2004.

[15] J. J. Chen, N. Y. Yu, D. G. Huang, B. T. Ann, and G. C. Chang, "Applying fuzzy logic to control cycling movement induced by functional electrical stimulation," *IEEE Trans. Rehabil. Eng.*, vol. 5, no. 2, pp. 158–169, 1997.

[16] M. Gföhler and P. Lugner, "Cycling by means of functional electrical stimulation," *IEEE Trans. Rehabil. Eng.*, vol. 8, no. 2, pp. 233–243, 2000.

[17] J. J. Abbas and H. J. Chizeck, "Neural network control of functional neuromuscular stimulation systems: computer simulation studies," *IEEE Trans. Biomed. Eng.*, vol. 42, no. 11, pp. 1117–1127, 1995.

[18] F. E. Zajac, "Muscle and tendon: Properties, models, scaling, and application to biomechanics and motor control," *CRC Crit. Rev. Biomed. Eng.,* vol. 17, no. 4, pp. 359411, 1989.

[19] W. K. Durfee and K. I. Palmer, "Estimation of force-activation, force-length, and force-velocity properties in isolated, electrically stimulated muscle," in *IEEE Transactions on Biomedical Engineering*, vol. 41, no. 3, pp. 205-216, March 1994, doi: 10.1109/10.284939.

[20] A. M. Gordon, A. F. Huxley, and F. J. Julian, "The variation in isometric tension with sarcomere length in vertebrate muscle fibres," *J. Physiol.*, vol. 184, no. 1, pp. 170–192, 1966.

[21] D. A. Winter, *Biomechanics and motor control of human movement*. Hoboken, NJ, USA: John Wiley & Sons, Inc., 2009.

[22] D. E. Anderson, M. L. Madigan, and M. A. Nussbaum, "Maximum voluntary joint torque as a function of joint angle and angular velocity: model development and application to the lower limb," *J. Biomech.*, vol. 40, no. 14, pp. 3105–3113, 2007.

[23] A. V. Hill, "The heat of shortening and the dynamic constants of muscle," *Proc. Biol. Sci.*, vol. 126, no. 843, pp. 136–195, 1938.

[24] M. Bellman, "Control of cycling induced by functional electrical stimulation: A switched systems theory approach," Ph.D. dissertation, University of Florida, 2015.

[25] E. S. Idsø, "Development of a mathematical model of a rider-tricycle system," Dept. of Engineering Cybernetics, NTNU, Tech. Rep., 2002.

[26] E. Henneman, G. Somjen, and D. O. Carpenter, "Functional significance of cell size in spinal motoneurons," *J. Neurophysiol.*, vol. 28, pp. 560–580, 1965.

[27] E. Langzam, Y. Nemirovsky, E. Isakov, and J. Mizrahi, "Partition between volitional and induced forces in electrically augmented dynamic isometric muscle contractions," *IEEE Trans. Neural Syst. Rehabil. Eng.*, vol. 14, no. 3, pp. 322–335, 2006.